Transactions of the Materials Research Society of Japan 24 [1] 23-26 (1999)

Influence of Higher-Harmonic Electric Field on Jump Phenomena of Current in Piezoelectric-Ceramic Vibrators

Keisuke Ishii, Takashi Yamada, Shinjiro Tashiro and Hideji Igarashi
Department of Electronic Engineering, The National Defense Academy,
1-10-20 Hashirimizu, Yokosuka, Kanagawa, 239-8686, Japan.
Fax: +81-486-44-5903, e-mail: kishii@cc.nda.ac.jp

When piezoelectric-ceramic vibrators with rectangular configuration were driven at high power levels, current-jump phenomena appeared. In order to investigate the origin of the phenomena, a theoretical calculation was done by means of an equivalent circuit equation including a nonlinear term due to 3rd harmonic electric field which comes from ferroelectric nonlinearity. The nonlinear coefficients in the equation were estimated from the power-law relation between the sample current and the harmonic electric field, and the coefficients were used in the calculation of jump current. The theoretical calculation values of currents well corresponded to the measured values of current jump phenomena. From this result, it was found that the jump phenomena are due to the generation of the 3rd harmonic electric field.
Key words: Jump phenomena, Nonlinear phenomena, Higher harmonic field, Piezoelectric ceramics, PZT

1. INTRODUCTION

For a more widely application of piezoelectric ceramics to high power use, it is indispensable to evaluate the origin and the generation mechanism of current-jump phenomena which is one of the main factors preventing the stable running under high power operation.[1,2] Recently, several studies taking notice of nonlinearity of piezoelectric materials have been reported to discuss the mechanism which induces the jump phenomena at around a resonance frequency.[3,4] Authors have also reported the generation of higher harmonic voltages which are caused by the nonlinearity of ferroelectric ceramics.[5,6] In addition, it is well known that 3rd order nonlinearities cause jump phenomena in mechanical resonance of vibrations[7] and in electrical resonance of LCR circuits[8]. In this paper, the 3rd harmonic electric field was discussed in regard to the current-jump phenomena.

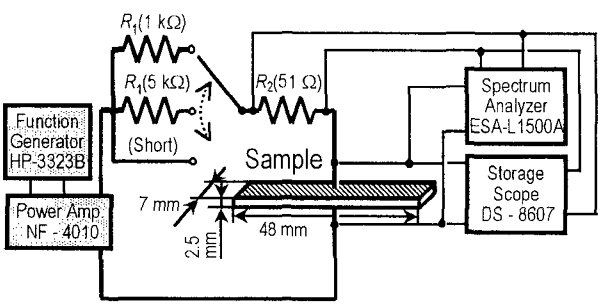

Fig. 1. Sample configuration and experimental setup.

2. EXPERIMENTAL

The observation and analysis of voltage and current of samples were performed using a measuring circuit as shown in Figure 1. The sample was driven with voltages of a precise sinusoidal waveform produced by a signal generator (Hewlett Packard, HP-3323B) and a power amplifier (NF Electric Instruments, NF-4010) at around the resonance frequency of length-extensional ½ λ mode vibration through series resistors R_1 and R_2. The series resistor, R_1 was inserted for the realization of constant current driving, while R_2 was inserted for monitoring the current. When the measurement was done by the constant-current method, the input current was kept constant by the series resistor R_1 of 1 kΩ or 5 kΩ during the measurements, because the resistance of the sample was about 100Ω at the resonance frequency. On the other hand, when measured by the constant-voltage method, the series resistor R_1 was removed from the measurement circuit (R_1= 0 Ω). The measurement circuit shown in Fig. 1 can be regarded as a circuit of constant-voltage driving. The waveforms of the sample voltage and current were monitored using a digital storage scope (IWATSU, DS-8607), and their analysis was performed using a spectrum analyzer (Hewlett Packard, ESA-L1500A). The details of the measurements method are described in previous papers.[5,6]

The composition of the prepared samples is as follows.

$0.95Pb(Zr_{0.51}Ti_{0.49})O_3$ - $0.05Pb(Sb_{0.5}Nb_{0.5})O_3$
+ 0.01 $MnCO_3$

The starting materials are extra-pure Pb_3O_4, ZrO_2, TiO_2, Sb_2O_3, Nb_2O_5 and $MnCO_3$. The sample was prepared by means of a conventional method.[5,6] The sample configuration was a rectangular bar with a size of 48 X 7 X 2.5 mm, as shown in Fig 1. The electromechanical coupling factor, mechanical quality factor, and elastic resonance frequency of the sample measured using an LF impedance analyzer (HP, 4192A) under a small signal field at room temperature, are k_{31}=0.35, Q_m=1270, and f_0=34.7 kHz, respectively. The sample was a 'hard-material' with a high mechanical quality factor.

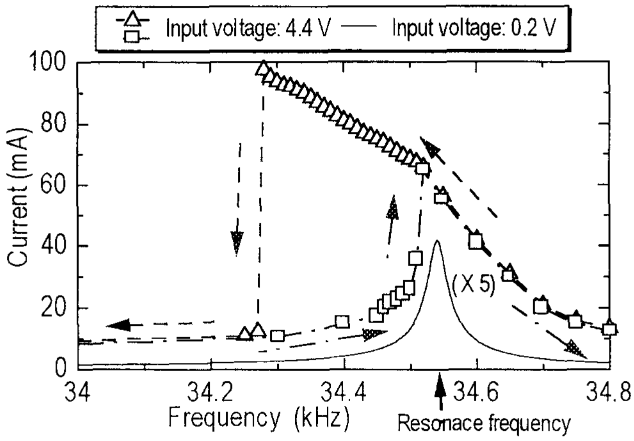

Fig. 2. Frequency response of current around the resonance frequency.

3. RESULTS AND DISCCSSION

The frequency response of current was studied when the samples were driven at a constant voltage around the resonance frequency. Figure 2 shows the relation between the frequency and the current when the sample was driven at constant voltages of 0.2 and 4.4 V. When the applied voltage is lower than 1 V, and when the current was lower than 10 mA, the typical resonance-current spectrum was observed as shown by the solid curve in Fig. 2, and the spectrum shape is

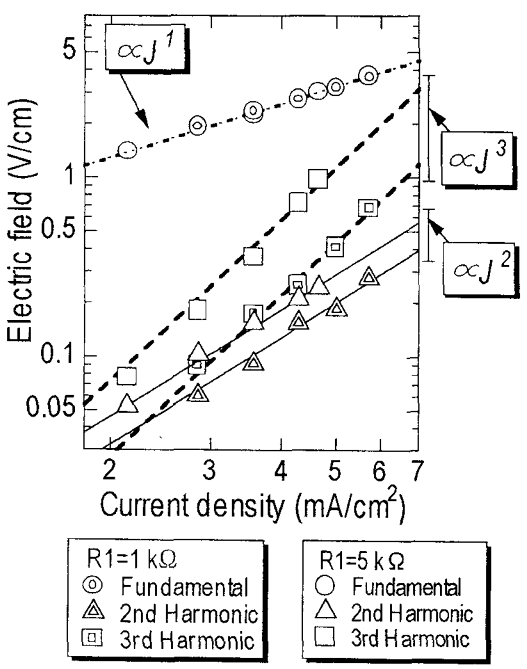

Fig. 3. Fundamental, 2nd, and 3rd harmonic fields as a function of current density at resonance frequency, when R_1 is 1 kΩ and 5 kΩ. The dotted line, solid line, and broken lines are drawn by assuming power law of ∝ J, ∝ J^2, and ∝ J^3, respectively.

symmetric with respect to the resonance frequency. With the increase of applied voltage, the shape of current spectrum became unsymmetric. In the lower frequency side than the resonance frequency, the rate of increase or decrease in the current became larger compared with the rate in the higher frequency side. When the current exceeded 20 mA with an increase in the applied voltage, a jump phenomenon appeared, and a hysteresis was observed in the current spectrum as shown by the plots in Fig. 2, while the voltage waves were maintained to be sinusoidal during the measurements.

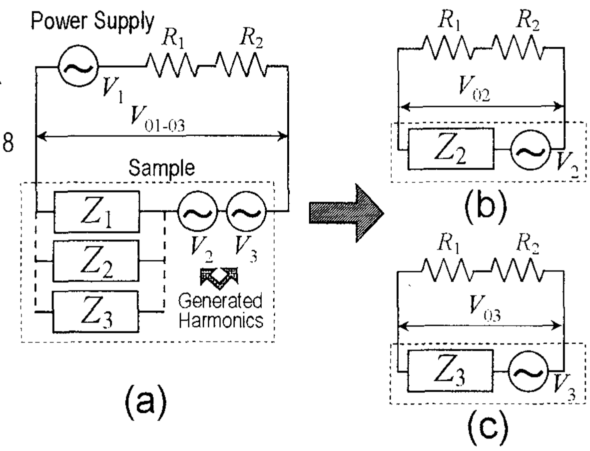

Fig. 4. Equivalent circuits containing the 2nd and 3rd harmonic voltages. (a) is the original circuit. (b) and (c) are circuits only for the 2nd and for the 3rd harmonic voltage, respectively.

It has been reported that the jump phenomenon with respect to frequency is observed in elastic materials having the property called 'soft spring' when they were driven at a constant stress.[7] The origin of the current-jump phenomenon had been considered to be the elastic softening from the analogy to the property of 'soft spring'.[2] However it is difficult to believe the mechanism of 'soft spring' in piezoelectric ceramics, since it has never been demonstrated by the experimental results. On the other hand, it has been also reported that nonlinearity of piezoelectric materials has a relation with the jump phenomena.[3, 4] Hence, we tried to explain the jump phenomenon by means of higher harmonic electric fields generated in piezoelectric ceramics instead of the softening.

We found that the higher harmonic voltages, which come from ferroelectric nonlinearity, were observed when piezoelectric ceramics vibrators were driven at high power levels around the resonance frequency with a constant-current method. Equation 1 expresses the observable electric field, which is based on the linear piezoelectric h-equation.

$$E = -hS + \beta D + E_h, \quad (1)$$

where, h are piezoelectric h constant, β, S, D, E are inverse permittivity, strain, electric flux density, applied field, and E_h is nonlinear electric field, respectively. By differentiating the Taylor series up to the S^4 and D^4 terms in Helmholtz's free energy

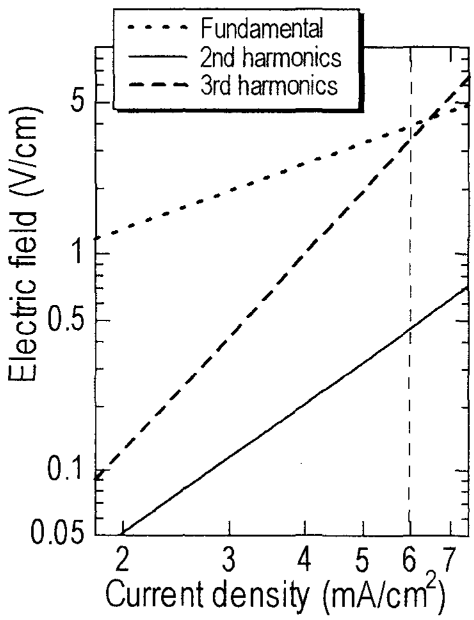

Fig. 5. Fundamental, 2nd, and 3rd harmonic fields corrected using Eq 4 as a function of current density.

with respect to D, E_h is described as following equation.

$$E_h = \gamma_1 D^2 + \gamma_2 SD + \gamma_3 S^2 + \xi_1 D^3 + \xi_2 D^2 S + \xi_3 DS^2 + \xi_4 S^3 \quad (2)$$

The $\gamma_{1\text{-}3}$ and $\xi_{1\text{-}4}$ are nonlinear coefficients. Here, it is difficult to estimate $\gamma_{1\text{-}3}$ and $\xi_{1\text{-}4}$. In addition, since the current due to strain S through piezoelectricity is quite larger than the current due to dumped capacitance at around the resonance frequency, D is nearly equal to the electric flux density due to only S at around the resonance frequency. This indicates that D can be regard as being proportional to S. Thus for convenience, E_h is described using only electric flux density as expressed by Eq 3.

$$E_h = \gamma D^2 + \xi D^3 \quad (3)$$

These 2nd and 3rd nonlinear terms are discussed through the comparison with the experimental results. Figure 3 shows the relationship between the current density and the 2nd and 3rd harmonic electric fields measured using the constant-current circuits with different R_1, 1 kΩ and 5 kΩ. In both cases of 1 kΩ and 5 kΩ, the magnitudes of 2nd and 3rd harmonics are proportional to the square and cube of current density, respectively. This fact agrees with the Eq 3. The magnitudes of the higher harmonics are larger when R_1 is 5 kΩ than when R_1 is 1 kΩ. This is caused by the difference of sample impedance for the 2nd and 3rd harmonic frequencies. Here, the equivalent measurement circuit containing the sample is assumed as shown in Fig. 4(a), where the sample impedance for the 2nd harmonic voltages V_2 is Z_2, and for the 3rd harmonic voltages V_3 is Z_3. When the impedances of the power supply for the higher harmonics are negligibly small, the equivalent circuits containing only 2nd harmonic voltage and containing only 3rd harmonic voltage are displayed as Fig. 4(b) and Fig. 4(c), respectively. Then, the relationship between the observable harmonic voltages V_{02}, V_{03} and the actual generated voltages V_2, V_3 are described by Eq 4.

$$V_{on} = \frac{R_1 + R_2}{R_1 + R_2 + Z_n} V_n \qquad (n=2, 3) \quad (4)$$

The 2nd resonance of the length-extensional ½λ mode vibration doesn't exist in the rectangular samples with electrodes of whole surfaces, and the 3rd resonance frequency doesn't preciously agree with the third times of the fundamental resonance frequency. From these facts, since the values of Z_2 and Z_3 are too large to be ignored compared to R_1+R_2, V_2 and V_3 are quite different from V_{02} and V_{03}. In order to know the precise values of V_2 and V_3, values of V_{02} and V_{03} observed when R_1 is 1 kΩ and 5 kΩ were substituted into Eq 4. Figure 5 shows the relationship between the current density and the actually generated harmonic electric fields which were obtained by dividing V_2 and V_3 by the sample thickness. The 2nd harmonic electric field is smaller about 1 order than the 3rd harmonic electric field in the region of the current density larger than 6 mA/cm² in which the jump phenomena are observed. This shows that the 2nd nonlinear term can be negligible as an origin of the jump phenomena, and that only the 3rd nonlinear term is considered to contribute to the jump phenomena. When γD^2 term is neglected in Eq 3, Eq 1 becomes the following equation.

$$E = -hS + \beta D + \xi D^3 \quad (5)$$

When the sample was driven at around the resonance frequency, the contribution of the dumped capacitance, namely, βD term in Eq 5 is also negligible. Since the hS term can be described using a series LCR circuit equation, the following circuit equation was obtained from Eq 5.

$$L\frac{di}{dt} + Ri + \frac{1}{C}\int idt + \xi'_{33}\left(\int idt\right)^3 = v \quad (6)$$

Here, the sample current $i = dq/dt$, electric charge q

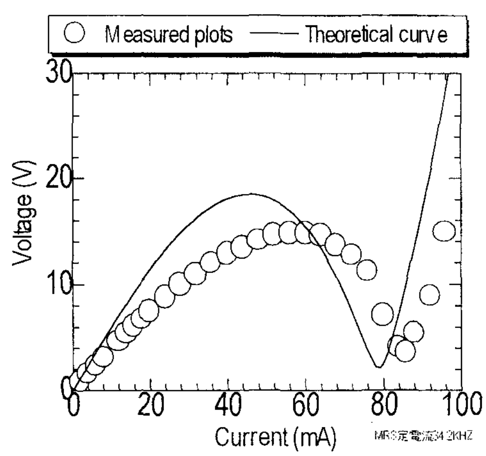

Fig. 6. Theoretical v_0-i_0 curve calculated using Eq 8 at constant frequency 34.2 kHz. The open circles show the experimental values measured with the constant current circuit when R_1 is 5 kΩ.

$= AD$, $\xi' = d\,\xi/A^3$, A is electrode surface area, d is sample thickness, L, C, R are inductance, resistance, capacitance of the equivalent circuit.

We tried to simulate the jump phenomenon shown in Fig. 2 using this equation. Although the current i is not exactly sinusoidal when the applied voltage is $v = v_0 \sin\omega t$, it was assumed that the current is $i = i_0 \sin(\omega t + \theta)$ as primary approximation. We substituted $v = v_0 \sin\omega t$ and $i_0 \sin(\omega t + \theta)$ into Eq 6. In addition, since the jump phenomenon is concerned with only the fundamental frequency component, the 3rd harmonics frequency component is negligible. Then, Eq 7 is obtained as follows.

$$v_0 \sin\omega t = \left(\omega L - \frac{1}{\omega C}\right) i_0 \cos(\omega t + \theta) + R i_0 \sin(\omega t + \theta) + \frac{3\xi'}{4\omega^3} i_0^{\,3} \cos(\omega t + \theta) = \sqrt{\left\{\left(\omega L - \frac{1}{\omega C}\right) i_0 + \frac{3\xi'}{4\omega^3} i_0^{\,3}\right\}^2 + (R i_0)^2} \times \sin(\omega t + \theta) \qquad (7)$$

Because the both sides of Eq .7 are equal in amplitude, the following equation is obtained. [7]

$$v_0 = \sqrt{\left\{\left(\omega L - \frac{1}{\omega C}\right) i_0 + \frac{3\xi'}{4\omega^3} i_0^{\,3}\right\}^2 + (R i_0)^2} \qquad (8)$$

The measured values were compared with the theoretical v_0-i_0 curve calculated using Eq 8. The values of L, C, and R, measured using an LF impedance analyzer (HP, 4192A) under a small signal field, are 143 mH, 149 pF, and 25 Ω, respectively. The absolute value of ξ' was 1.3 x 10^{21} V/A^3/s, and this value was decided by the relation between the 3rd harmonic electric field and the current density in Fig. 5. In addition, the sign of ξ' was found to be negative from the observed phase difference between the fundamental voltage and the 3rd harmonic voltage. The white circles in Fig. 6 show the values measured using the constant-current measurement circuit with R_1 of 5 kΩ at the constant frequency of 34.2 kHz. The calculated curve is similar to the behavior shown by the measured values. This suggests that the above assumptions used for derivation of Eq 8 are appropriate.

To simulate the jump phenomena, Eq 8 was transformed into Eq 9.

$$\frac{3\xi'_{33}}{4\omega^3} i_0^{\,3} = \left(\omega L - \frac{1}{\omega C}\right) i_0 \pm \sqrt{v_0^{\,2} - R^2 i_0^{\,2}} \qquad (9)$$

Since it is difficult to analytically solve Eq 9 for the current, the theoretical values of ω-i_0 curve were obtained by graphically solving it. The theoretical plots agree well with the experimental broken lines in Fig. 7. Thus, it was found that the 3rd harmonic electric field causes the current-jump phenomenon.

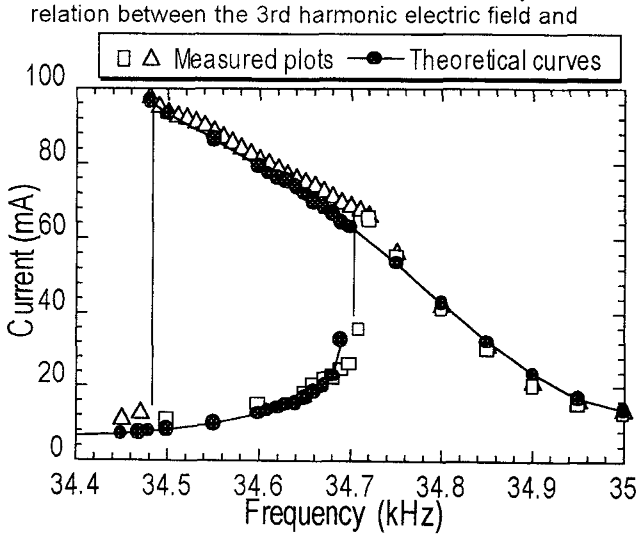

Fig. 7. Theoretical ω-i_0 curve of the jump phenomena calculated using Eq 9.

4. CONCLUSION

When the piezoelectric-ceramic vibrators of a rectangular configuration with electrodes of whole surfaces were driven at high power levels, the large 3rd harmonic electric field due to the ferroelectric nonlinearity was observed. It was found that this harmonic electric field induces the jump phenomena of current around the resonance frequency. This was confirmed by the theoretical calculation using the equivalent circuit including a nonlinear term due to the 3rd harmonic electric field.

References

1) T. Wada, "Analysis on Jumping Phenomenon of Ceramic Vibrator", In *Proceedings of the 1998 IEICE General Conference*, Hiratsuka, 1998, No. A-11-6, 289. (in Japanese)
2) "Piezoelectric Ceramics and Its Applications", Denpa-Shinbun Co., Tokyo (1974) pp. 38-41. (in Japanese)
3) R. Perez and A. Albareda, *J. Acoust. Soc. Am.*, **100**, 3561-69 (1996).
4) N. Aurelle, D. Guyomar, C. Richard, P. Gonnard, and L. Eyraud, *Ultrasonic*, **34**, 187-91 (1996).
5) K. Ishii, N. Akimoto, S. Tashiro, and H. Igarashi, *J.Ceram. Soc. Japan*, **106**, 555-58 (1998).
6) K. Ishii, N. Akimoto, S. Tashiro, and H. Igarashi, *Jpn. J. Appl. Phys.*, **37**, 5330-33 (1998).
7) O. Taniguchi, "New edition Industrial Oscillation Study", Corona Publishing Co., Tokyo (1977) pp. 140-57. (in Japanese)
8) K. Morisawa, "Alternating Current Theory", Denki-Shoin Co., Tokyo (1987) pp. 401-07. (in Japanese).

(Received December 11, 1998; accepted February 28, 1999)